



Fuzzy-Genetic Algorithm-Based Direct Power Control Strategy for DFIG

E. Heydari^{*(C.A.)}, M. Rafiee* and M. Pichan**

Abstract: Among a multitude of diverse control methods proposed for doubly fed induction generator (DFIG) based-wind energy conversion systems, direct power control (DPC) method has demonstrated superior dynamic performance and robustness in presence of disturbances. However, DPC is not a flawless method and shortcomings like necessity for high sampling frequency, high-speed sensors and less noise-affected sampling circuit need to be mitigated by utilizing fuzzy controllers. Parameter setting in a fuzzy controller plays a vital role, especially under non-ideal grid conditions. In this paper, a fuzzy-genetic algorithm-based direct power control (FGA-DPC) method is proposed for DFIG, while, the parameters of the fuzzy controller are optimized by genetic algorithm. The objective of the optimization is to minimize the stator active and reactive power errors to increase the precision of reference tracking. The objectives of the controller are also optimizing active power absorption based on the zone of operation and adjustment of reactive power according to grid requirements. The proposed method improves the overall precision and speed of transient response as well as significantly reducing power oscillations under non-ideal grid conditions. Finally, to demonstrate the effectiveness of the proposed method, extensive simulations are performed in Matlab/Simulink under different conditions.

Keywords: Wind Energy Conversion System, DFIG, Direct Power Control, FGA-DPC.

Nomenclature

φ_s, φ_r	Stator and rotor flux vectors
I_s, I_r	Stator and rotor current vectors
V_s, V_r	Stator and rotor voltage vectors
L_s, L_r	Stator and rotor self-inductances
L_m	Mutual inductance
R_s, R_r	Stator and rotor resistances

Subscripts

s, r	Stator, rotor
d, q	Synchronous d-q axis

Superscript

s	Synchronous reference frame
-----	-----------------------------

Iranian Journal of Electrical and Electronic Engineering, 2018.

Paper first received 01 November 2017 and accepted 24 May 2018.

* The authors are with the Department of Electrical Engineering, Shahid Beheshti University, Tehran, Iran.

E-mails: e_heydari87@ymail.com and m_rafi@pwut.ac.ir.

** The author is with the Department of Electrical Engineering, Amirkabir University of Technology, Tehran, Iran.

E-mail: m.pichan@aut.ac.ir.

Corresponding Author: E. Heydari.

1 Introduction

IN the past decades, with increasing use of renewable energy resources, it has been reported that the cumulative wind capacity installed worldwide at the end of 2021 would reach over 800 GW [1]. Among the generators used in variable speed wind turbines, doubly fed induction generators (DFIG) have been considered to a greater extent [2-5]. So, various control methods have been proposed for DFIGs. Among these methods, direct power control (DPC) offers many advantages include: fast dynamic response, simplicity in calculations, and robustness against machine parameter mismatches [6-9]. The DPC method presented in [10], imposes some drawbacks such as variable switching frequencies. Although several methods have been proposed with fixed switching frequency [11, 12], these methods require high sampling frequency to show good steady state and transient performance. High sampling frequency means high-speed sensors and sampling circuits which must be enough robust against external noise, which leads to increased cost of the system. So in [13, 14], direct power control method based on fuzzy

controller has been proposed. This controller provides advantages such as reduced dependence on accurate model of the system, robustness against change in the machine parameters, and robustness against noise. In [13], DPC is presented based on discrete space vector modulation (DSVM), and a fuzzy controller is used to reduce power ripples. The switching table used in this method makes it necessary for reducing the power ripples to have high switching frequency and many vector definitions. In [14], the fuzzy-based DPC is used to control the active and reactive powers. However, this method restricts its control on fixed power gained from the turbine. Besides, it does not consider the turbine dynamics connected to the DFIG and its analytical information. On the other hand, due to the nonlinearity and complexity of the system, it is not easy to find the optimal scale factors for the controller, which was not addressed in this reference.

Since finding the optimal fuzzy control coefficients plays an important role in the accuracy of the response and lower power errors, optimization algorithms can be used for the automatic adjustment of these coefficients. Among these algorithms, genetic algorithm (GA) because of its advantages such as wide solution space, ease of discovering global optimum, resistance against becoming trapped in local optimum and ease of implementation is highly attractive and usable [15-17]. In this paper, a new direct power control strategy for DFIG in wind energy conversion systems is proposed. The proposed strategy is fuzzy-genetic algorithm-based direct power control (FGA-DPC). The aim of optimizing the scale factors by the genetic algorithm is to minimize the stator active and reactive power error in reference tracking. Also, by the appropriate setting of reference power, the power absorbed from the turbine is adjusted with respect to the performance zone. In other words, the purpose of the controller is to adjust reactive power according to grid requirements and optimize the active power with the minimum error.

2 System Description

The mechanical power of the wind turbine (P_t) is a function of the available power in the wind ($P_v=1/2 \pi \rho R^2 v^3$). The mechanical power of the wind turbine can be obtained based on (1):

$$P_t = P_v C_p (\lambda, \beta_p) = \frac{1}{2} \pi \rho R^2 v^3 C_p (\lambda, \beta_p) \tag{1}$$

where v is the wind speed, ρ is the air density, and R is the blade length, respectively. On the other hand and after some calculations, the mechanical torque of the turbine can be obtained as follow [18].

$$T_t = \frac{P_t}{\omega_m} = \frac{1}{2} \times \frac{\pi \rho C_t (\lambda) R^3 v^2}{K_{gb}} \tag{2}$$

where $C_t (\lambda)$ is the torque coefficient of the turbine. When the pitch angle β_p is constant, C_p is a nonlinear function of λ and has a unique maximum value for $\lambda = \lambda_{opt}$ that is shown in Fig. 1(a). The relationship between wind speed and produced power by the turbine is shown in Fig. 1(b). The turbine performance is useful just in two regions; in zone 2 (partial load zone), in which the target would be to absorb maximum power from the wind. In zone 3 (full load zone), in which it is necessary to limit the absorbing power to the rated value by controlling pitch angle of the blades or electrical circuit.

2.1 Dynamic Model of the DFIG

The dynamic behavior of the DFIG can be explained based on the five differential equations [14].

$$V_s^s = R_s I_s^s + \frac{d\varphi_s^s}{dt} + j \omega_s \varphi_s^s \tag{3}$$

$$V_r^s = R_r I_r^s + \frac{d\varphi_r^s}{dt} + j (\omega_s - \omega_m) \varphi_r^s \tag{4}$$

$$\varphi_s^s = L_s I_s^s + L_m I_r^s \tag{5}$$

$$\varphi_r^s = L_m I_s^s + L_r I_r^s \tag{6}$$

$$T_e = \frac{3}{2} p (\varphi_{ds} I_{qs} - \varphi_{qs} I_{ds}) = T_t - J \frac{d\omega_m}{dt} \tag{7}$$

where ω_s and ω_m are stator and mechanical angular frequencies, respectively. In addition, T_e denotes the electrical torque of the generator, T_t is the torque produced by the wind turbine, J is the inertia of the whole rotating parts, and p is the number of pole pairs.

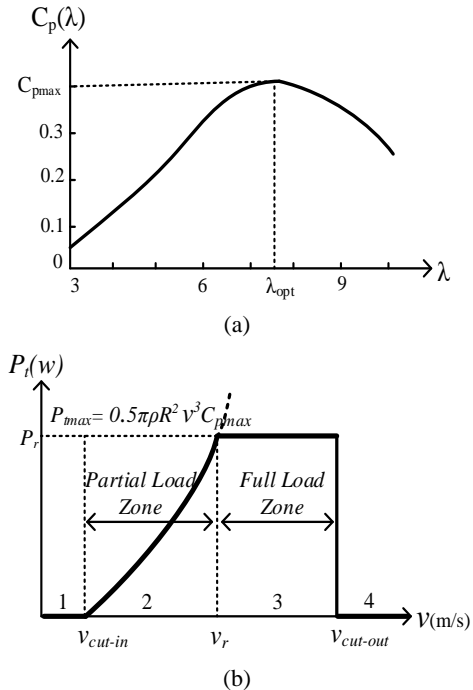


Fig. 1 Wind energy conversion system: a) Curve of C_p based on λ , $C_p (\lambda) = 9.5946(12 / \lambda - 1)e^{(-20/\lambda)}$, ($\beta_p = 0$) and b) Zones of operation for a wind turbine.

3 Controller

3.1 Active and Reactive Power Control

Using (5) and (6), the stator current in the synchronous reference frame is obtained as follows:

$$I_s^s = \frac{L_r \varphi_s^s - L_m \varphi_r^s}{L_s L_r - L_m^2} = \frac{\varphi_s^s}{\sigma L_s} - \frac{L_m \varphi_r^s}{\sigma L_s L_r};$$

$$\sigma = \frac{L_s L_r - L_m^2}{L_s L_r} \quad (8)$$

Under ideal grid voltages, amplitude and rotating speed of the stator flux are fixed, so $d\varphi_s^s/dt = 0$. Therefore, neglecting the stator resistance, the stator voltage equation can be simplified as (9).

$$V_s^s = V_{ds} + jV_{qs} = j\omega_s \varphi_s^s \quad (9)$$

By alignment of d -axis of synchronous reference frame and the stator flux vector, active and reactive power can be expressed as follow:

$$P_s = k \sigma V_{qs} \varphi_{qr} \quad (10)$$

$$Q_s = -k \sigma V_{qs} \left(\frac{L_r V_{qs}}{L_m \omega_s} + \varphi_{dr} \right) \quad (11)$$

where $k_\sigma = \frac{3}{2} L_m / (\sigma L_s L_r)$. The Eq. (10) and (11) imply that the injected active and reactive power to the grid can be controlled by φ_{qr} and φ_{dr} , respectively. Now, the rotor flux derivation at each small sampling time (T_s) can be written as follows:

$$\frac{d\varphi_r^s}{dt} = \frac{\varphi_r^s(k+1) - \varphi_r^s(k)}{T_s}$$

$$= V_r^s - R_r I_r^s(k) - j(\omega_s - \omega_m) \varphi_r^s(k) \quad (12)$$

After decomposing (12) and regardless of the rotor resistance, d and q components of the rotor flux in the $(k+1)$ sample instant are obtained and given in (13) and (14).

$$\varphi_{dr}(k+1) = \varphi_{dr}(k) + T_s V_{dr}(k) + T_s (\omega_s - \omega_m) \varphi_{qr}(k) \quad (13)$$

$$\varphi_{qr}(k+1) = \varphi_{qr}(k) + T_s V_{qr}(k) - T_s (\omega_s - \omega_m) \varphi_{dr}(k) \quad (14)$$

In a dead beat theory with two sample delays, the target is to calculate the switching signal at instant $k+1$ based on the current values (instant k). As a result, all of the values at instant $k+1$ are considered the reference values, so:

$$P_{ref}(k) = P(k+1) \quad (15)$$

$$Q_{ref}(k) = Q(k+1) \quad (16)$$

Again, by considering (15) and (16) and substituting (13) and (14) in (10) and (11), the rotor reference voltage values in the synchronous reference frame are obtained as follows [14]:

$$V_{qr}(k) = \frac{1}{T_s} \frac{\Delta P_s}{k_\sigma V_{qs}(k)} + (\omega_s - \omega_m) \varphi_{dr} \quad (17)$$

$$V_{dr} = \frac{1}{T_s} \frac{-\Delta Q_s}{k_\sigma V_{qs}(k)} - (\omega_s - \omega_m) \varphi_{qr} \quad (18)$$

Therefore, the stator active and reactive power control occurs through q and d components of the rotor voltage (V_{qr} and V_{dr}), respectively.

To generate the reference voltages of the rotor side converter, reference values of the stator active power at the speed higher and lower speeds than the rated speed are needed. When the machine is operated in the maximum power absorption ($C_p = C_{pmax}$, $\lambda = \lambda_{opt}$), the torque can be stated in proportion to the square of the rotor speed as follows:

$$T_{opt} = \frac{\pi \rho R^5 C_{pmax}}{2 k_{gb}^3 \lambda_{opt}^3} \omega_m^2 = k_o \omega_m^2 \quad (19)$$

where $k_o = \frac{\pi \rho R^5 C_{pmax}}{2 k_{gb}^3 \lambda_{opt}^3}$. On the other hand, when the

wind speed is high and power production is limited to the rated value, the torque equation can be obtained as (20).

$$T_r = \frac{P_r}{\omega_m} \quad (20)$$

where P_r is rated power. Therefore, the value of P_{sref} is proportional to:

$$P_{sref} = \frac{T_{ref} \omega_s}{p} \quad (21)$$

where T_{ref} is the amount of reference torque which is dependent on the performance zone presented in (19) and (20). Finally, the amount of Q_{sref} is considered according to the needs of the grid.

3.2 Design of FGA-DPC

In this study, in order to control active and reactive powers, two independent fuzzy controllers are used. Active power controller gets the stator active power error (e_p) and its integration ($\int e_p$) as input and produces q -axis rotor voltage (V_{qr}) as output. On the other hand, reactive power controller inputs are stator reactive power error (e_q) and its integration ($\int e_q$) and its output is d -axis rotor voltage (V_{dr}). The structures of the proposed controllers are shown in Fig. 2(a).

Each input and output variable in the fuzzy plane is

introduced with seven membership functions. These membership functions are shown in Fig. 2(b) and fuzzy rules are shown in Table 1.

An example of these rules is considered below:

If e_p (e_q) is x and i_s is y , then is w .

In the proposed controller, Mamdani inference engine, min-max fuzzy communication system, and defuzzification method of centroid are used [18]. In the structures of the proposed controllers shown in Fig. 2(a), $K_{E,P}$, $K_{IE,P}$, $K_{E,Q}$, and $K_{IE,Q}$ are input scale factors of the active and reactive power controllers, respectively. Besides, $K_{P,P}$, $K_{I,P}$, $K_{P,Q}$, and $K_{I,Q}$ are output scale factors of the controllers. These coefficients are adjusted by genetic algorithm because of its advantages.

3.3. Genetic Algorithm

Genetic algorithm, instead of working on a solution and optimizing it in the next iteration, works on the set of solutions simultaneously and gradually converges toward an optimal point. Thus, the probability of falling into the local minimum trap is too low.

The steps of the GA algorithm implementation for the proposed method are summarized as follows:

1. Start: At this stage, the initial population is randomly generated according to the production method given in (22).

$$\text{Initial population} = (K_{hi} - K_{lo})K_{norm} + K_{lo} \quad (22)$$

where K_{hi} is the largest number in a range of variable, K_{lo} is the smallest number in a range of variable, and K_{norm} is the normalized value of variable. The initial population size is considered equal to 20.

2. Fitness: The merit of each chromosome is evaluated based on the objective function which is defined as Minimize J_{total} :

$$J_{total} = \int (W_1 |P_{sref} - P_s| + W_2 |Q_{sref} - Q_s|) dt \quad (23)$$

where W_1 and W_2 are the weighting coefficients.

3. Selection: Two parents are selected from a population based on their fitness (more fitness, more chance of being selected).

4. Crossover: At this stage, the crossover operators act on the chromosomes of the parents. Each pair of parents is considered below:

$$\begin{aligned} \text{Parent 1} &= [P_{m1} P_{m2} \dots P_{m\alpha} \dots P_{mN_{var}}] \\ \text{Parent 2} &= [P_{d1} P_{d2} \dots P_{d\alpha} \dots P_{dN_{var}}] \\ \alpha &= \text{roundup}(\text{random} * N_{var}) \end{aligned} \quad (24)$$

where m and d are the indexes of the mother and father chromosomes. Also, N_{var} is the number of variables

which equal to 8. The chromosomes selected in (24) are combined to produce children by single-point crossing. Finding the random point to single-point crossing is shown in (25) [19].

$$\begin{aligned} P_{new1} &= P_{m\alpha} - \beta [P_{m\alpha} - P_{d\alpha}] \\ P_{new2} &= P_{d\alpha} + \beta [P_{m\alpha} - P_{d\alpha}] \end{aligned} \quad (25)$$

where β is a random value within the range (1,0). The final stage in crossing is completing children as shown in (26):

$$\begin{aligned} \text{offspring 1} &= [P_{m1} P_{m2} \dots P_{new1} \dots P_{dN_{var}}] \\ \text{offspring 2} &= [P_{d1} P_{d2} \dots P_{new2} \dots P_{mN_{var}}] \end{aligned} \quad (26)$$

5. Mutation: At this stage, mutation process with probability 0.2 acts on the chromosomes of crossover and, by changing the bits of chromosomes, creates a way to enter new information.

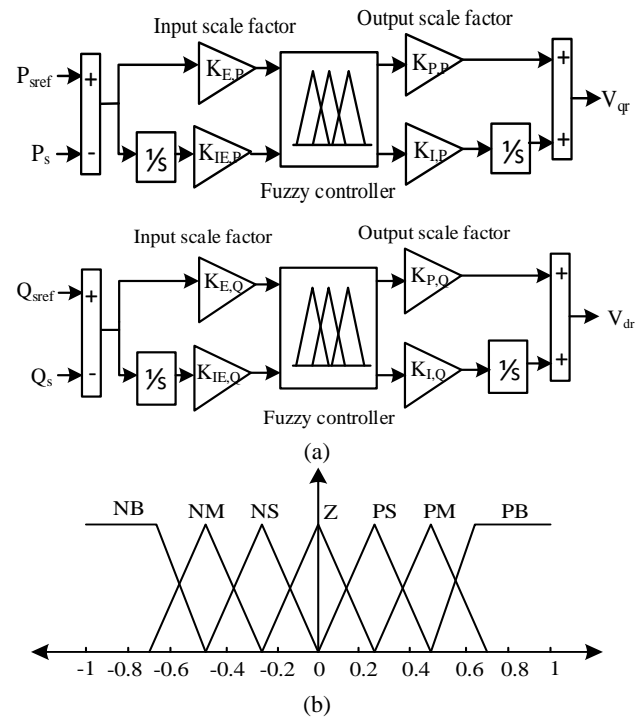


Fig. 2 The proposed active and reactive power controllers: a) Controllers block diagram and b) Normalized membership functions.

Table 1 Rule base of fuzzy controller.

Δe	NB	NM	NS	Z	PS	PM	PB
e	Z	PS	PM	PB	PB	PB	PB
NS	Z	PS	PM	PB	PB	PB	PM
NM	NS	Z	PS	PM	PB	PB	PS
NB	NM	NM	Z	PM	PM	PB	Z
NB	NB	NM	NS	Z	PS	PM	NS
NB	NB	NB	NM	NS	Z	PS	NM
NB	NB	NB	NB	NM	NS	Z	NB

6. Accepting: Then, the children are placed in a new population.

7. Replace: At this stage, the new population is selected to enter the next stage algorithm, which is done by comparing the fitness of chromosomes.

8. Test: At this stage, all the new population will be assessed. If the conditions for termination of the algorithm are provided, the algorithm ends; otherwise, the population as initial population will be used for the next stage.

In the optimization process via GA, the goal is to minimize J (fitness function) in order to minimize the stator active and reactive power error to precisely track the reference values. For this purpose, optimization variables are considered as $K_{P,P}, K_{I,P}, K_{IE,P}$ and $K_{E,P}$ for active power controller and $K_{P,Q}, K_{I,Q}, K_{E,Q}$, and $K_{IE,Q}$ for reactive power controller. So there are 8 optimization variables in genetic algorithm. The detailed block diagram for fuzzy controller optimized by genetic algorithm is shown in Fig. 3.

Actually, the fitness function is obtained from simulated system in Simulink and it has been called using "sim" command in genetic algorithm to capture the results from Simulink file.

4 Simulations Results

In order to evaluate the performance of the proposed control system under various conditions, extended simulations in Matlab/Simulink are carried out. The scheme of the simulated system is shown in Fig. 4(a). The parameters of the simulated system are given in Table 2. A wind speed profile is considered as shown in Fig. 4(b), which guarantees the operation of the system in both acceptable zones.

In order to provide a better evaluation and show the superior performance of the proposed FGA-DPC controller, the results of implementing the proposed controller are compared to those of a PI controller under various condition that gains of PI controller is also set by genetic algorithm [20]. The convergence of the objective function in terms of the number of generations is presented in Fig. 5, demonstrating that, at the end of the algorithm, the objective function reaches its optimal value. The scale factors of proposed controller are given in Table 3.

In order to provide a better evaluation and show the superior performance of the proposed FGA-DPC controller, the results of implementing the proposed controller are compared to those of a PI controller under various condition that gains of PI controller is also set by genetic algorithm [20]. The convergence of the objective function in terms of the number of generations is presented in Fig. 5, demonstrating that, at the end of the algorithm, the objective function reaches its optimal value. The scale factors of proposed controller are given in Table 3.

4.1 Operation under Ideal Grid Condition

The first study is related to evaluating the performance of the control system in normal grid conditions. In this case, the reference active power is prepared according to (21) in order to achieve the control purposes. The results for active and reactive powers are shown in Fig. 6. Also, stator and rotor currents are shown in Fig. 7. Accordingly, the results indicate precise and appropriate reference tracking of the proposed controller with lower errors, which leads to improved power absorption process from wind turbine and also supplies the required reactive power.

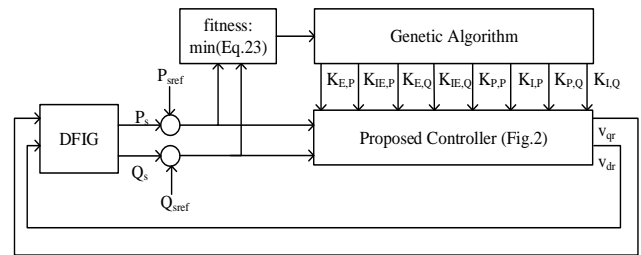


Fig. 3 The detailed block diagram of fuzzy controller optimized by genetic algorithm.

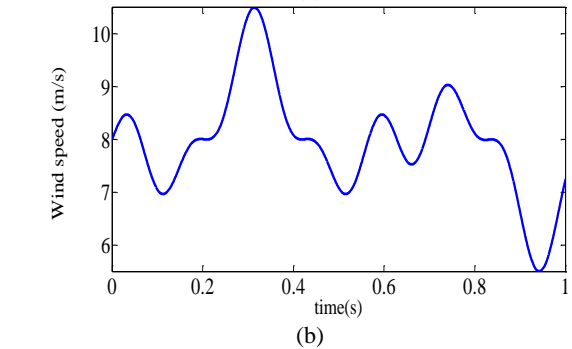
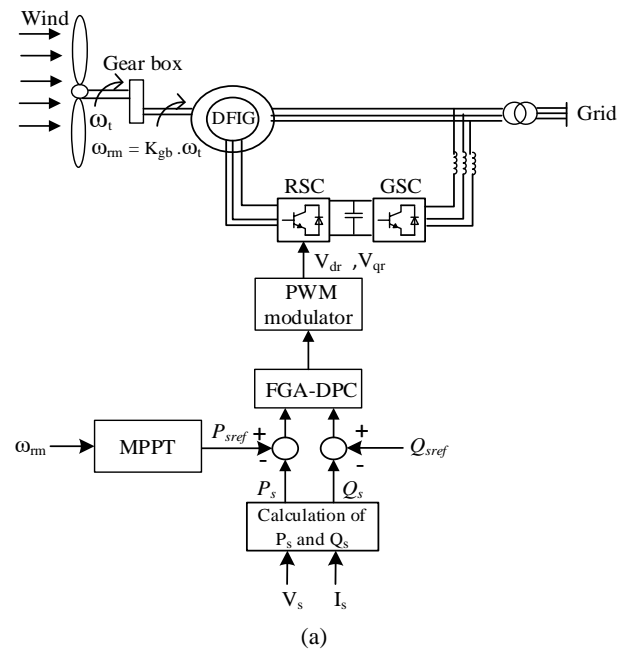


Fig. 4 The simulated system by the proposed controller: a) Scheme of the simulated system and b) Wind speed profile.

Table 2 Parameters of the simulated system.

WT's Parameters	
J	3.662 kg.m ²
k_{gb}	25
C_{pmax}	0.4
λ_{opt}	7.5
R	7.3 m
DFIG's Parameters	
P_{nom}	50 Hp
R_s	82 mΩ
R_r	228 mΩ
L_s	35.5 mH
L_r	35.5 mH
L_m	34.7 mH
P	2
Grid's Parameters	
V_s	$460\sqrt{\frac{2}{3}}$ V
f_s	60 Hz

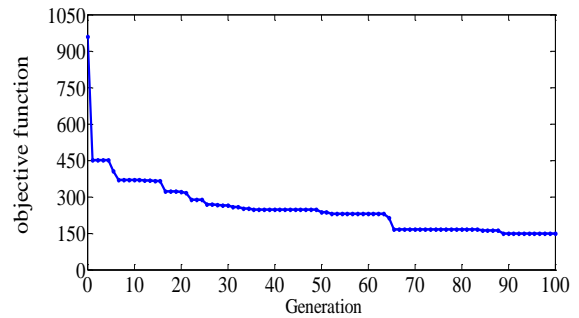
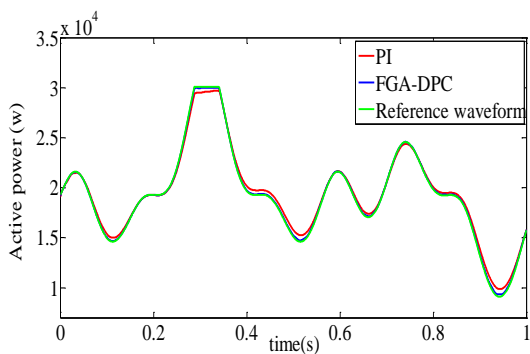


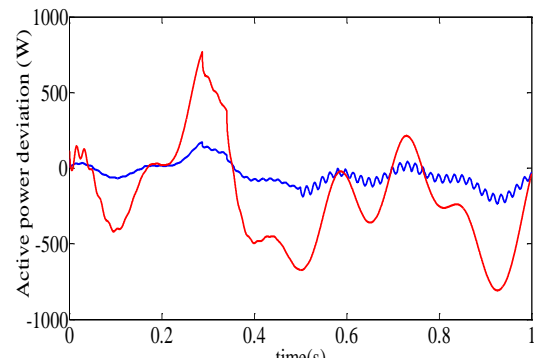
Fig. 5 Convergence of objective function.

Table 3 Parameters of proposed controller.

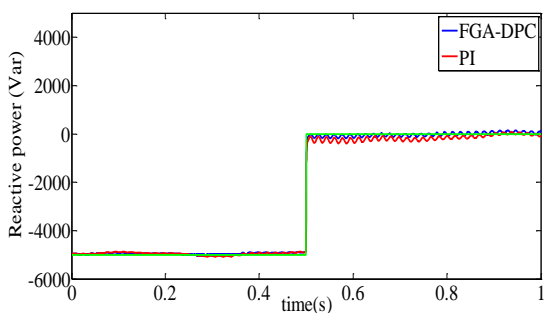
$K_{E,P}$	$K_{IE,P}$	$K_{E,Q}$	$K_{IE,Q}$
1.65e-4	3.32e-5	1.67e-4	9.60e-5
$K_{P,P}$	$K_{I,P}$	$K_{P,Q}$	$K_{I,Q}$
95.71	66.28	37.53	56.49



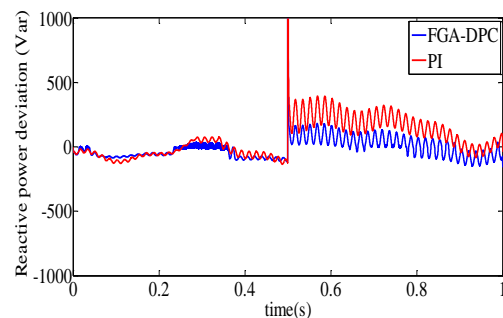
(a)



(b)

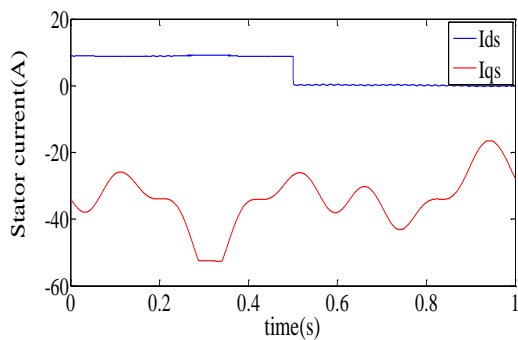


(c)

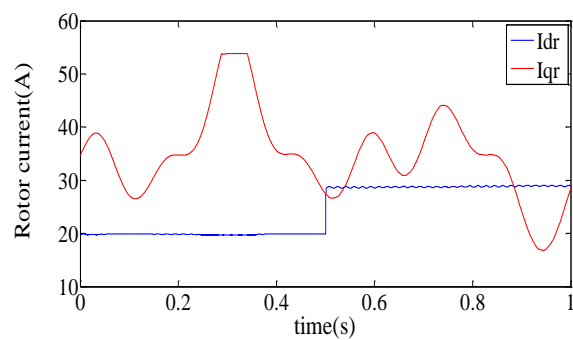


(d)

Fig. 6 Performance of FGA-DPC and PI controllers in normal grid conditions.



(a)



(b)

Fig. 7 Stator and rotor currents in normal grid conditions.

4.2 Operation under Non-Ideal Grid Voltage

4.2.1 Operation under Grid Voltage Dip

In this study, the grid voltage dip condition is considered on the operation of the DFIG. This fault is a 20% voltage dip in 200 ms. For gaining a better assessment of the transient performance, the wind and reactive powers are considered to be constant and the results are shown in Fig. 8(a). The results reveal that the use of the proposed controller not only is effective in fast oscillation damping of the active and reactive power, but also makes the system stable earlier which improves the whole stability of the system. It is worth to be mentioned that the THD value of the grid current is 1.3% under this condition for the proposed method which verify the effectiveness of the proposed method.

4.2.2 Operation under Imbalanced Grid Voltages

In order to study the behavior of the controller under the condition of imbalanced grid voltage, three-phase voltages of the grid with regard to the sequence of positive and negative sequence components are considered in (27). The performance of the controllers in this mode for tracking the stator powers considering $k = 0.01$ is shown in Fig. 8(b).

$$\begin{aligned}
 v_{ag} &= V_m \cos(\omega_s t) + kV_m \cos(\omega_s t) \\
 v_{bg} &= V_m \cos\left(\omega_s t - \frac{2\pi}{3}\right) + kV_m \cos\left(\omega_s t + \frac{2\pi}{3}\right) \\
 v_{cg} &= V_m \cos\left(\omega_s t + \frac{2\pi}{3}\right) + k \cos\left(\omega_s t - \frac{2\pi}{3}\right)
 \end{aligned}
 \tag{27}$$

The results show a significant reduction in power oscillations by using the fuzzy genetic controller in comparison to the case using PI controller. Also, for better comparison, the value of power ripple is obtained from (28) and the results for the proposed method, conventional DPC method [14] and PI control methods are shown in Table 4. Accordingly, it is confirmed that the proposed method not only provides better performance than PI controllers but also, it also shows lower power ripple compared to the conventional DPC method.

$$\Delta s (\%) = \sqrt{\frac{\Delta P^2 + \Delta Q^2}{P_{ref}^2 + Q_{ref}^2}} \times 100
 \tag{28}$$

5 Conclusion

To precisely regulate the active and reactive powers of the DFIG in wind energy conversion systems, the new

Table 4 Power ripple $\Delta s\%$ as a function of voltage imbalance.

k	FGA	PI	Conventional DPC [14]
0.01	3.70	6.79	5.4
0.03	11.30	19.58	16.7

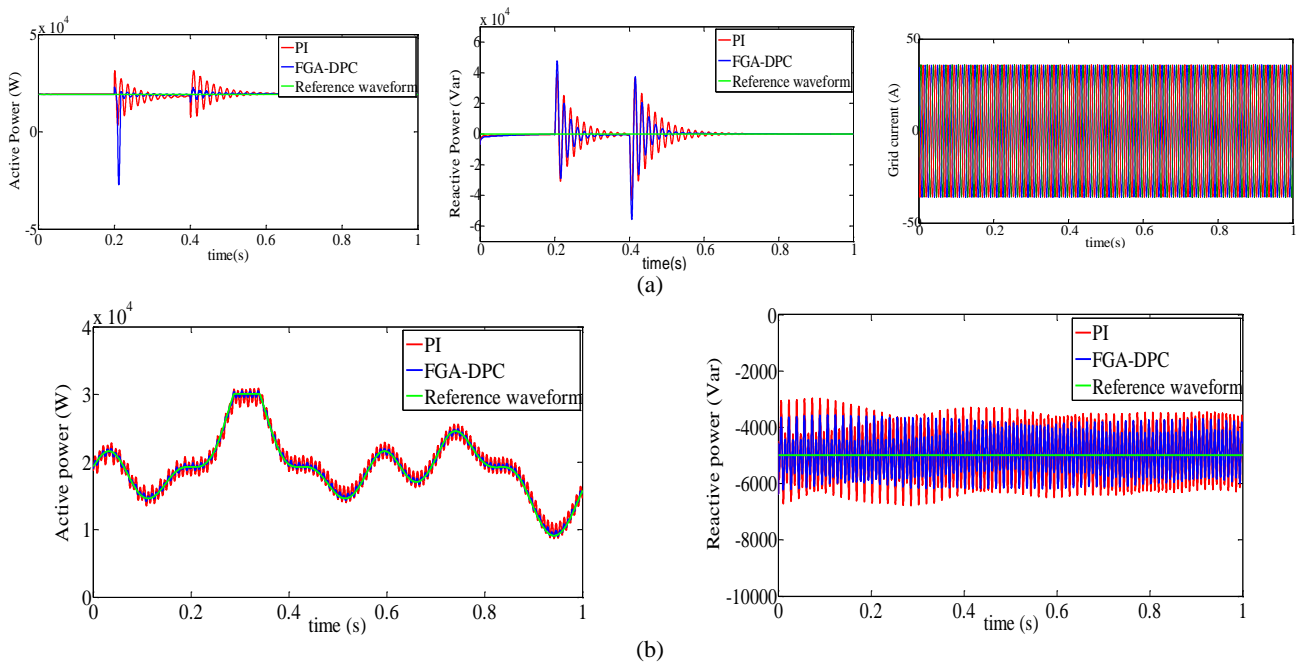


Fig. 8 Performance of FGA-DPC and PI controllers under non ideal grid voltages: a) Under grid voltage dip and b) Under imbalanced grid voltages.

fuzzy genetic-based direct power control method was proposed in this paper. The genetic algorithm was used for the optimal adjustment of coefficients of the fuzzy controller in order to minimize power error and increase the response precision. In addition, based on the zones of wind turbine operation, different objectives were considered. In order to study the control performance, extensive simulations were performed under different wind speeds and different grid conditions and the results were compared with those of a PI controller. By implementing the proposed controller, the reference tracking error and power oscillations were decreased and the oscillation of the active and reactive power was damped after disturbance clearance in a faster rate.

References

- [1] Y. Kumar, J. Ringenberg, S. Shekara Depuru, V. K. Devabhaktuni, J. W. Lee, E. Nikolaidis, B. Andersen and A. Afjeh "Wind energy: trends and enabling technologies," *Renewable and Sustainable Energy Reviews*, Vol. 53, pp. 209–224, 2016.
- [2] J. Carroll, A. McDonald and D. McMillan, "Reliability comparison of wind turbines with DFIG and PMG drive trains," *IEEE Transactions on Energy Conversion*, Vol. 30, No. 2, pp. 663–670, 2015.
- [3] R. Pour Ebrahim, S. Tohidi and A. Younesi, "Sensorless model reference adaptive control of DFIG by using high frequency signal injection and fuzzy logic control," *Iranian Journal of Electrical and Electronic Engineering*, Vol. 14, No. 1, pp. 11–21, Mar. 2018.
- [4] J. Hu, B. Wang, W. Wang, H. Tang, Y. Chi and Q. Hu, "Small signal dynamics of DFIG-based wind turbines during riding through symmetrical faults in weak AC grid," *IEEE Transactions on Energy Conversion*, Vol. 32, No. 2, pp. 720–730, 2017.
- [5] H. Li and Z. Chen, "Overview of different wind generator systems and their comparisons," *IET Renewable Power Generation*, Vol. 2, No. 2, pp. 123–138, 2008.
- [6] Y. Djeriri, A. Meroufel, A. Massoum and Z. Boudjema, "A comparative study between field oriented control strategy and direct power control strategy for DFIG," *Journal of Electrical Engineering*, 2014.
- [7] A. Djoudi, S. Bacha, H. Chekireb, H. Iman-Eini and C. Boudinet, "Adaptive sensorless SM-DPC of DFIG-based WECS under disturbed grid: study and experimental results," *IEEE Transactions on Sustainable Energy*, Vol. 9, No. 2, pp. 570–581, 2018.
- [8] L. Li, H. Nian, L. Ding and B. Zhou, "Direct power control of DFIG system without phase-locked loop under unbalanced and harmonically distorted voltage," *IEEE Transactions on Energy Conversion*, Vol. 33, No. 1, pp. 395–405, 2018.
- [9] S. K. Sahoo, "Comparison of SVM and DPC for reactive power control of DFIG based wind energy systems," *International Journal of Renewable Energy*, Vol. 11, No. 1, pp. 1–8, 2016.
- [10] L. Xu and P. Cartwright, "Direct active and reactive power control of DFIG for wind energy generation," *IEEE Transactions on Energy Conversion*, Vol. 21, No. 3, pp. 750–758, 2006.
- [11] D. Zhi and L. Xu, "Direct power control of DFIG with constant switching frequency and improved transient performance," *IEEE Transactions on Energy Conversion*, Vol. 22, No. 1, pp. 110–118, 2007.
- [12] D. Zhi, L. Xu and B. W. Williams, "Model-based predictive direct power control of doubly fed induction generators," *IEEE Transactions on Power Electronics*, Vol. 25, No. 2, pp. 341–351, 2010.
- [13] M. V. Kazemi, M. Moradi and R. V. Kazemi, "Minimization of powers ripple of direct power controlled DFIG by fuzzy controller and improved discrete space vector modulation," *Electric Power Systems Research*, Vol. 89, pp. 23–30, 2012.
- [14] M. Pichan, H. Rastegar and M. Monfared, "Two fuzzy-based direct power control strategies for doubly-fed induction generators in wind energy conversion systems," *Energy*, Vol. 51, pp. 154–162, 2013.
- [15] T. D. Vrionis, X. I. Koutiva and N. A. Vovos, "A genetic algorithm-based low voltage ride-through control strategy for grid connected doubly fed induction wind generators," *IEEE Transactions on Power Systems*, Vol. 29, No. 3, pp. 1325–1334, 2014.
- [16] A. Zemmit, S. Messalti and A. Harrag, "A new improved DTC of doubly fed induction machine using GA-based PI controller," *Ain Shams Engineering Journal*, 2017.
- [17] A. M. Abdelsalam and M. El-Shorbagy, "Optimization of wind turbines siting in a wind farm using genetic algorithm based local search," *Renewable Energy*, Vol. 123, pp. 748–755, 2018.
- [18] S. Heshmatian, D. Arab Khaburi, M. Khosravi, A. Kazemi, "Development and analysis of a novel multi-mode MPPT technique with fast and efficient performance for PMSG-based wind energy conversion systems," *Iranian Journal of Electrical and Electronic Engineering*, Vol. 14, No. 1, pp. 37–48, Mar. 2018.

- [19] F. Herrera, M. Lozano and J. L. Verdegay, "Tuning fuzzy logic controllers by genetic algorithms," *International Journal of Approximate Reasoning*, Vol. 12, No. 3, pp. 299–315, 1995.
- [20] B. P. Ganthia, V. Agarwal, K. Rout and M. K. Pardhe, "Optimal control study in DFIG based wind energy conversion system using PI & GA," in *International Conference on Power and Embedded Drive Control (ICPEDC)*, pp. 343–347, 2017.



E. Heydari received her B.Sc. in Electrical Engineering from University of Razi, Kermanshah, Iran, in 2012. She finished her M.Sc. in Electrical Engineering at Shahid Beheshti University, Tehran, Iran, in 2015. She is currently working toward her Ph.D. at Tarbiat Modares University. Her research interests include power electronics and its applications in renewable energies.



M. Rafiee was born in Iran in 1967. He received his B.Sc. degree from the Sharif University of Technology in 1981, M.Sc. degree from KNT University of Technology in 1996 and Ph.D. Degree from Iran University of Science and Technology (IUST) in 2006, all in Electrical Engineering. He is currently Assistant Professor in Shahid Beheshti University (SBU) and his current research interests include modeling and analysis of Distributed Generation and Renewable energy.



M. Pichan received his B.Sc. in Electronics Engineering from University of Isfahan, Isfahan, Iran, in 2010. He finished his M.Sc. in Electrical Engineering at Amirkabir University of Technology, Tehran, Iran, in 2012. He received his Ph.D. degree in Electrical Engineering from Amirkabir University of Technology, Tehran, Iran, in 2017. He is currently Assistant Professor at the Iranian Research Institute of Electrical Engineering working on medium and high power converters design. His research interests include rectifiers, inverters, and power electronics and their applications in renewable energies.



© 2018 by the authors. Licensee IUST, Tehran, Iran. This article is an open access article distributed under the terms and conditions of the Creative Commons Attribution-NonCommercial 4.0 International (CC BY-NC 4.0) license (<https://creativecommons.org/licenses/by-nc/4.0/>).